Control of the Geometry of a Railway Track: Measurements of Defects and Theoretical Simulation

KONSTANTINOS S. GIANNAKOS
Civil Engineer PhD, Fellow/Life-Member ASCE
108 Neoreion str., Piraeus 18534 GREECE

Abstract: — The Railway track, is simulated as a beam on elastic foundation with damping. The motion of a vehicle is simulated by the 2nd order differential equation of motion; the input to the system "vehicle-rail" is the form of the Track Geometry which "acts" as a "signal". The defects with short and long wavelength influence the value of the dynamic component of the acting loads on the railway track and they are recorded in the frame of the Quality Control of the Railway Track. A sensitivity analysis is performed for both cases of defects.

Keywords: Track Defects, Long and Short Wavelength, Fourier Transforms, Track Recording.

Received: April 19, 2022. Revised: November 14, 2022. Accepted: December 14, 2022. Published: December 31, 2022.

International Journal on Applied Physics and Engineering, Volume 1, 2022
https://wseas.com/journals/articles.php?id=7722
https://wseas.com/journals/ape/2022/a22ape-011(2022).pdf

1. Introduction

The railway track is usually modeled as a continuous beam on elastic support. Train circulation is a random dynamic phenomenon and, depending on the different frequencies of the loads it imposes, there is a corresponding response of the track superstructure. At the instant when an axle passes from the location of a sleeper, a random dynamic load is applied on the sleeper. The theoretical approach for the estimation of the dynamic loading of a sleeper requires the analysis of the total load acting on the sleeper to individual component loads-actions, which, in general, can be divided into: (a) the static component of the load, and the relevant reaction/action per support point of the rail (sleeper) and (b) the dynamic component of the load, and the relevant reaction/action per support point of the rail (sleeper). The static component of the load on a sleeper, in the classical sense, refers to the load undertaken by the sleeper when a vehicle axle at standstill is situated exactly on top of the sleeper. For dynamic loads with low frequencies the load is essentially static. The static load is further analyzed into individual component loads: the static reaction/action on a sleeper due to wheel load and the semi-static reaction/action due to cant deficiency ([1]). The dynamic component of the load of the track depends on the mechanical properties (stiffness, damping) of the system "vehicle-track" (Fig. 1), and on the excitation caused by the vehicle's motion on the track.

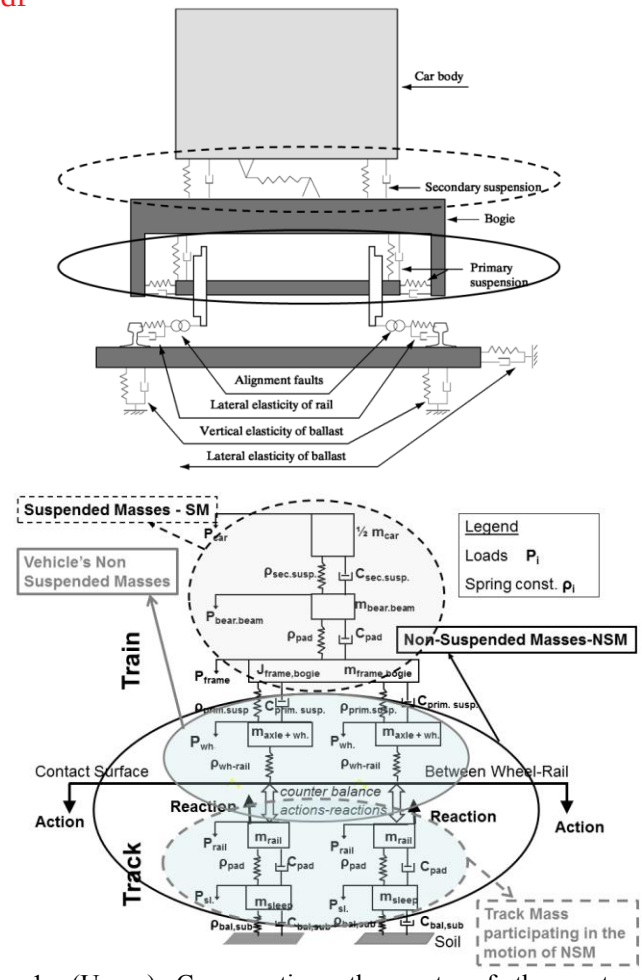

Fig. 1. (Upper) Cross-section: the parts of the system "Railway Vehicle-Railway Track"; (lower) this system as an ensemble of springs and dashpots.

The response of the track to the aforementioned excitation results in the increase of the static loads on the superstructure.

The dynamic load is primarily caused by the motion of the vehicle's Non-Suspended (Unsprung) Masses, which are excited by track geometry defects, and, to a smaller degree, by the effect of the Suspended (sprung) Masses. In order to formulate the theoretical equations for the calculation of the dynamic component of the load, the statistical probability of exceeding the calculated load -in real conditions- should be considered, so that the corresponding equations would refer to the standard deviation (variance) of the load ([1]]; [2]). The track defects are classified in short wavelenth defects and long wavelength defects. An article for "Modeling the Influence of the Short Wavelength Defects in a Railway Track on the Dynamic Behavior of the Non-Suspended Masses" appeared ([3]); it refers to the consecutive defects, not isolated. In the present paper the dynamic component of the acting loads, for the long wavelength defects, is – mainly – investigated through the second order differential equation of motion of the Non Suspended Masses of the Vehicle and specifically the transient response of the reaction/ action on each support point (sleeper) of the rail.

2. Masses in the System "Vehicle-railway Track"

The railway vehicles consist of (a) the car-body, (b) the primary and the secondary suspension with the bogie between them and (c) the axles with the wheels (Fig. 1-upper). In general the mass of the (c) case under the primary suspension is the Non Suspended Mass of the vehicle. The heaviest vehicles are the locomotives which are "motive units" and have electric motors on the axles and/or the frame of the bogie. In Fig. 2-left a locomotive with three-axle bogie is depicted while the three axle bogie with the springs of the primary and secondary suspensions is depicted in Fig. 2-lower.

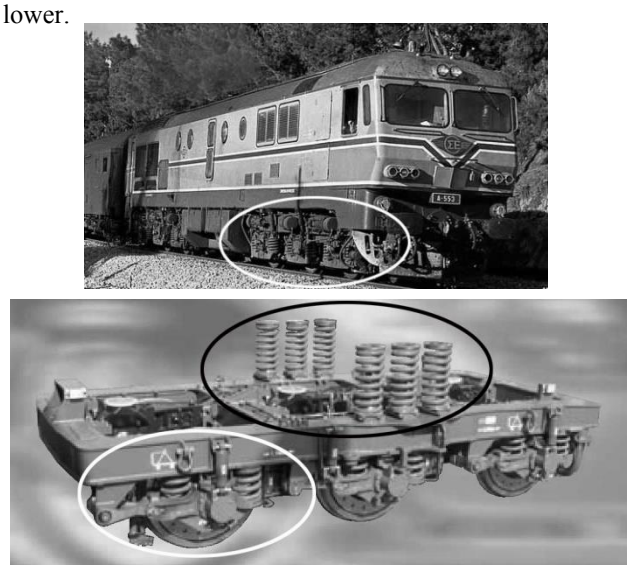

Fig. 2: (upper) Electropoutere type diesel locomotive of the Greek railways, with three-axle bogies of 20,8 t/axle and NSM 5,08 t/axle, on a railway track; the three-axle bogie is marked with the white ellipse; (lower) a three-axle bogie in detail: in the white ellipse the primary suspension and in the black ellipse the secondary suspension are depicted.

Electric motors are either suspended totally from the frame of the bogie or they are suspended on the frame of the bogie at one end and supported on the axle at the other end. In the second case the electric motor is semi-suspended (Fig. 3) and a part of it is considered also as Non Suspended Mass, as it will be clarified below.

If we try to approach mathematically the motion of a vehicle on a railway track, we will end up with the model shown in Fig. 1-lower, where both the vehicle and the railway track are composed of an ensemble of masses, springs and dashpots.

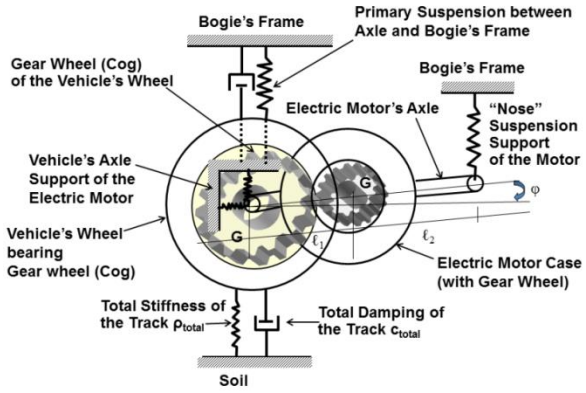

Fig. 3: Schematic depiction of an Electric Motor "semi-suspended" from the bogie's frame at one end ("Nose" suspension) and supported on the vehicle's axle at the other end.

As we can observe, the car body is supported by the secondary suspension that includes two sets of "springs-dashpots", seated on the frame of the bogie (Fig. 1-left and Fig. 3-right). The loads are transferred to the truss and the side frames of the bogie. Underneath the bogie there is the primary suspension, through which the bogie is seated onto the carrying axles and the wheels. Below the contact surface, between the wheel and the rail, the railway track also consists of a combination of masses-springs-dampers that simulates the rail, the sleepers, the elastic pad, the rail fastenings, the ballast and the ground.

The masses of the railway vehicle located under the primary suspension (axles, wheels and a percentage of the electric motor weight in the case of locomotives) are the Non Suspended Masses (N.S.M.) of the Vehicle, that act directly on the railway track without any damping at all. Furthermore a section of the track mass (m_{TRACK}) also participates in the motion of the vehicle's Non Suspended Masses, which also highly aggravates the stressing on the railway track (and on the vehicle too) ([1]; [2]].

The defects of the rail running table, a wave in space of random nature, impose a forced oscillation on the Non Suspended Masses of the vehicle; their form constitutes a forcing excitation. From the form of the rail running table the forcing period or frequency can be calculated.

The remaining vehicle masses are called Suspended Masses (S.M.) or Sprung Masses: the car-body, the secondary suspension, the frame of the bogie, a part of the electric motor's weight and the primary suspension.

3. Simulation of the Railway Track and the Second Order Differential Equation of Motion

The theoretical analysis of a railway track is based mainly in Winkler's theory ([4]), which models it as an infinite beam on elastic foundation. In European literature it is also referred to as Zimmermann's theory ([5]). The elastic foundation of the railway track can be simulated by a large number of closely spaced translational springs and the following equation is valid ([3]; [6]):

$$EJ\frac{\partial^4 y}{\partial x^4}+\rho_1\cdot\frac{\partial^2 y}{\partial x^2}+k_1\cdot z=0 \quad (1)$$

in the absence of external force, or:

$$EJ\frac{\partial^4 y}{\partial x^4}+\rho_1\cdot\frac{\partial^2 y}{\partial x^2}+k_1\cdot y=-Q\cdot\delta(x) \quad (2)$$

with the presence of external force.

In these equations y is the deflection of the beam, ρ1 is the mass of the track participating in the motion, k1 the viscous damping of the track, J is the moment of inertia of the rail, E is the modulus of elasticity of the rail, Q the force/ load from the wheel (when the force is present) and δ(x) the deflection of the rail at the contact point between wheel and rail.

The solution of equations (1) and (2) becomes challenging if we want to take into account all the parameters according to professor J. Alias ([7]). However, if we make some simplifying hypotheses we will be able to approximate the influence of certain parameters provided that we will verify the theoretical results with experimental measurements. Apparently having in mind the tests on track under operation, performed by the European Railways and the International Union of Railways (U.I.C.), professor J. Eisenmann states already since 1988 that, the -based on Zimmermann's theory- methods give results correspondent at the average of the measured on track values, for track's loading and stressing, as well as track's deflection ([8]). Consequently, the level of maximum values is dependent on the possibility of occurrence –mainly– of the dynamic component of the acting load.

If the acting load is determined, then the Action-Reaction on each support point (sleeper) of the rail will be determined too. The system "railway vehicle-railway track" operates based on the classical principles of physics: equivalence of Action-Reaction between the vehicle and the track. It is a dynamic stressing of random, vertical form.

The loading of the railway track from a moving vehicle consists of:

(a) the static component of the load (static load of the vehicle's axle), as given by the rolling stock's producer.

(b) the semi-static component of the load (due to cant or superelevation deficiency at curves, which results in non-compensated lateral acceleration).

(c) the component of the load from the Non-Suspended Masses of the vehicle (the masses that are not damped by any suspension, because they are under the primary suspension of the vehicle), which is a dynamic load by its nature and

(d) the component of the load from the Suspended Masses of the vehicle, that is a damped force component of the total action on the railway track and it is also a dynamic load.

On each support point of the rail (sleeper) a reaction/action is applied due to the distribution of the acting load to the adjacent sleepers (support points of the rail) because of the total elasticity/total static stiffness coefficient of the track. For the static and the semi-static components of the load these reactions/actions are given from the Eqns (2a) and (2b), as derived from the solution of the differential equation of motion. But for the dynamic component of the load a modelling of the motion of the Non Suspended Masses should be performed.

Finally the differential equation is transformed to the following equation connecting the deflection of the continuous beam and the bending moment ([3]; [6]):

$$\frac{d^4 y}{dx^4}=-\frac{1}{E\cdot J}\cdot\frac{d^2 M}{dx^2} \quad (3)$$

where y is the deflection of the rail, M is the bending moment, J is the moment of inertia of the rail, and E is the modulus of elasticity of the rail. From the differential equation (3), it is derived that the reaction of a sleeper R_{static} is (since the load is distributed along the track over many sleepers):

$$R_{stat}=\frac{Q_{wheel}}{2\sqrt{2}}\cdot\sqrt[4]{\frac{\ell^3\cdot\rho}{E\cdot J}}\Rightarrow\frac{R_{stat}}{Q_{wheel}}=\bar{A}=\bar{A}_{stat}=\frac{1}{2\sqrt{2}}\cdot\sqrt[4]{\frac{\ell^3\cdot\rho}{E\cdot J}} \quad (4a)$$

where Q_{wheel} the static wheel load, ℓ the distance among the sleepers, E and J the modulus of elasticity and the moment of inertia of the rail, R_{stat} the static reaction/action on the sleeper, and ρ reaction coefficient of the sleeper which is defined as: ρ=R/y, and is a quasi-coefficient of the track elasticity (stiffness) or a spring constant of the track. $\bar{A}=\bar{A}stat$ equals to R_{stat}/Q_{wheel}, which is the percentage of the acting (static) load of the wheel that the sleeper undertakes as (static) reaction. In reality, the track consists of a sequence of materials –in the vertical axis– (substructure, ballast, sleeper, elastic pad/ fastening, rail), that are characterized by their individual coefficients of elasticity (static stiffness coefficients) ρ_i (Fig. 4).

$$\rho_i=\frac{R}{y_i}\Rightarrow y_i=\frac{R}{\rho_i}\Rightarrow y_{total}=\sum_{i=1}^{\nu}y_i\Rightarrow y_{total}=\sum_{i=1}^{\nu}\frac{R}{\rho_i}\Rightarrow$$
$$\Rightarrow y_{total}=R\cdot\sum_{i=1}^{\nu}\frac{1}{\rho_i}\Rightarrow\frac{1}{\rho_{total}}=\sum_{i=1}^{\nu}\frac{1}{\rho_i} \quad (5)$$

where ν is the number of various layers of materials that exist under the rail -including rail– elastic pad, sleeper, ballast etc. Five main parameters of the layers are used: ρ_{rail}, ρ_{pad}, $\rho_{sleeper}$, $\rho_{ballast}$ and $\rho_{subgrade}$, that is finally the number of springs ν=5. The semi-static Load is produced by the centrifugal acceleration exerted on the wheels of a vehicle that is running in a curve with cant deficiency, given by the following equation ([1]; [7]; [9]):

$$Q_\alpha=\frac{2\cdot\alpha\cdot h_{CG}}{e^2}\cdot Q_{wheel} \quad (5\text{-}1)$$

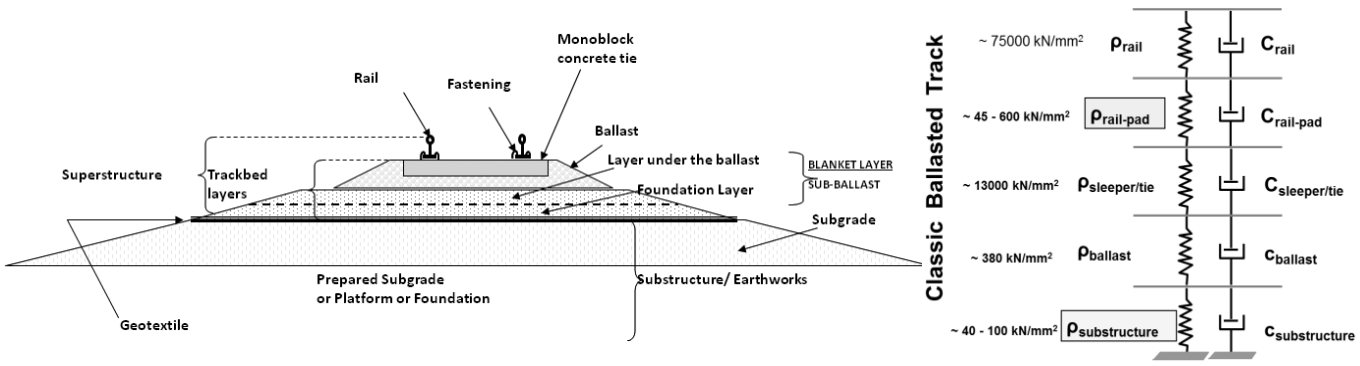

Fig. 4 Cross-section of Track and Characteristic Values.

where α is the cant deficiency, h_{CG} the height of the center of gravity of the vehicle from the rail head and e the track gauge. The semi-static Action/Reaction is derived by the multiplication of Q_α by the $\bar{A}_{stat}$. So equation (2a) is transformed to:

$$\frac{R_{stat}}{Q_{wheel}+Q_\alpha}=\bar{A}=\bar{A}_{stat}=\frac{1}{2\sqrt{2}}\cdot\sqrt[4]{\frac{\ell^3\cdot\rho}{E\cdot J}}\Rightarrow R_{stat}=\left(Q_{wheel}+Q_\alpha\right)\cdot$$

$$\cdot\frac{1}{2\sqrt{2}}\cdot\sqrt[4]{\frac{\ell^3\cdot\rho}{E\cdot J}}\Rightarrow R_{stat}=\left(Q_{wheel}+Q_\alpha\right)\cdot\bar{A}_{stat} \quad (2b)$$

4. Modeling the Motion of the Non Suspended Masses in the System "Railway Vehicle-railway Track"

The Suspended (sprung) Masses of the vehicle –masses situated above the primary suspension– create forces with very small influence on the wheel's trajectory and on the system's excitation. This enables the simulation of the track as an elastic media with damping, as shown in Fig. 5 (see relevantly [3]; [10]), and also the modelling of the motion of the Non Suspended Masses of a railway vehicle on it. Forced oscillation is caused by the irregularities of the rail running table (like an input random signal) –which are represented by n–, in a gravitational field with acceleration g, whilst the total deflection of the rail's running table, due to the wheel's passage, is y. As already described, there are two suspensions on the vehicle for passenger comfort purposes: primary and secondary suspension. Moreover, a section of the mass of the railway track participates in the motion of the Non-Suspended (Unsprung) Masses of the vehicle. These Masses are situated under the primary suspension of the vehicle.

If the random excitation (track irregularities) is given, it is difficult to derive the response, unless the system is linear and invariable. In this case the input signal can be defined by its spectral density and from this we can calculate the spectral density of the response. The theoretical results confirm and explain the experimental verifications performed in the former British railway network ([11]; relevant results in [7], p.39, 71 and also in [3]; [6]).

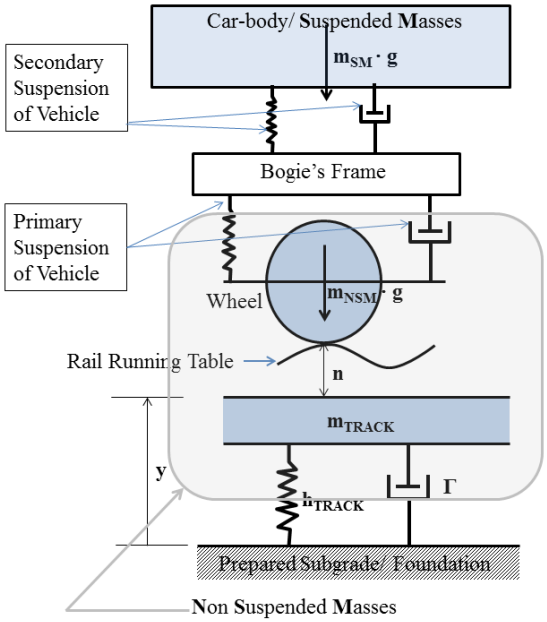

Fig. 5 Model of a rolling wheel, on the rail running table: n is the ordinate of the defect of the rail running table, y is the deflection of the rail.

If the random excitation (track irregularities) is given, it is difficult to derive the response, unless the system is linear and invariable. In this case the input signal can be defined by its spectral density and from this we can calculate the spectral density of the response. The theoretical results confirm and explain the experimental verifications performed in the former British railway network ([11]; relevant results in [7], p.39, 71 and also in [3]; [6]).

The equation for the interaction between the vehicle's axle and the track-panel becomes ([3]; [6]; [12]):

$$\left(m_{NSM}+m_{TRACK}\right)\cdot\frac{d^2y}{dt^2}+\Gamma\cdot\frac{dy}{dt}+h_{TRACK}\cdot y=$$

$$=-m_{NSM}\cdot\frac{d^2n}{dt^2}+\left(m_{NSM}+m_{SM}\right)\cdot g \quad (6)$$

where: m_{NSM} the Non-Suspended (Unsprung) Masses of the vehicle, m_{TRACK} the mass of the track that participates in the motion, m_{SM} the Suspended (Sprung) Masses of the vehicle that are cited above the primary suspension of the vehicle, Γ damping constant of the track (for its calculation see [13];

[14]), $h_{TRACK}=\rho_{dynamic}$ the total dynamic stiffness coefficient of the track, n the fault ordinate of the rail running table and y the total deflection of the track.

The phenomena of the wheel-rail contact and of the wheel hunting, particularly the equivalent conicity of the wheel and the forces of pseudo-glide, are non-linear. In any case the use of the linear system's approach is valid for speeds lower than the Vcritical≈500 km/h. The integration for the non-linear model (wheel-rail contact, wheel-hunting and pseudoglide forces) is performed through the Runge Kutta method ([7], p.94-95, 80; [15], p.98; [16], p.171, 351). Consequently for all operational speeds in High Speed Railway Lines up to now the linear model, which we use, is quite reliable.

The defects of the rail running table are categorized in short wavelength defects and long wavelength defects. The analysis and investigation of the Eqn (6), for consecutive short wavelength defects (e.g. the rail surfaces corrugation, of wavelength of some centimeters), was presented in [3]. The long wavelength defects are difficult to be measured, since sometimes, their wavelength overpass the measurements' base, which is determined by the distance between the measuring vehicle's axles. In this article the long wavelength defects are modelled, analyzed and investigated.

The dynamic component of the acting load consists of the action due to the Sprung or Suspended Masses (SM) and the action due to the Unsprung or Non Suspended Masses (NSM) of the vehicle. To the latter a section of the track mass is added, that participates in its motion ([13]; [14]). The Suspended (Sprung) Masses of the vehicle –masses situated above the primary suspension (Fig. 1)– apply forces with very small influence on the trajectory of the wheel and on the excitation of the system. This enables the simulation of the track as an elastic media with damping which takes into account the rolling wheel on the rail running table ([3]; [17]; [18]). Forced oscillation is caused by the irregularities of the rail running table (simulated by an input random signal) – which are represented by n–, in a gravitational field with acceleration g. There are two suspensions on the vehicle for passenger comfort purposes: primary and secondary suspension. Moreover, a section of the mass of the railway track participates in the motion of the Non-Suspended (Unsprung) Masses of the vehicle. These Masses are situated under the primary suspension of the vehicle.

We approach the matter considering that the rail running table contains a longitudinal fault/ defect of the rail surface. In the above equation, the oscillation of the axle is damped after its passage over the defect. Viscous damping, due to the ballast, enters the above equation under the condition that it is proportional to the variation of the deflection dy/dt. To simplify the investigation, if the track mass (for its calculation see ([13]; [14]) is ignored -in relation to the much larger Vehicle's Non Suspended Mass- and bearing in mind that y+n is the total subsidence of the wheel during its motion (since the y and n are added algebraically), we can approach the problem of the random excitation, based on a cosine defect (V< Vcritical=500 km/h):

$$\eta = a\cdot\cos\omega = a\langle\cos\left(2\pi\cdot\frac{V\cdot t}{\lambda}\right) \quad (7)$$

The second order differential equation of motion is:

$$m_{NSM}\frac{d^2z}{dt^2}+\Gamma\cdot\frac{dz}{dt}+h_{TRACK}\cdot z=-m_{NSM}\cdot a\cdot\omega^2\cdot\cos(\omega t) \quad (8)$$

The complete solution of which using polar coordinates is ([6], p.199 and ch.3):

$$z=\underbrace{A\cdot e^{-\zeta\omega_n t}\cdot\sin\left(\omega_n t\sqrt{1-\zeta^2}-\varphi\right)}_{transient-part}+\underbrace{a\cdot B\cdot\cos(\omega t-\varphi)}_{steady-state-part} \quad (9)$$

where, the first term is the transient part and the second part is the steady state part.

5. The Specific Case of an Isolated Track-defect

The modelling described in paragraph 4, give equations to calculate the actions on track depending on the parametrical analysis of the conditions on the railway track. In order to approach the long wavelength defects, we begin by trying to relate the depth (sagittal) of an isolated defect to the dynamic component of the load. We neglect the steady state part of Eqn (9):

$$a\cdot B\cdot\cos(\omega t-\varphi) \quad (10)$$

We focus herein on the transient part of the load, that is the term:

$$A\cdot e^{-\zeta\omega_n t}\cdot\sin\left(\omega_n t\sqrt{1-\zeta^2}-\varphi\right) \quad (11)$$

We investigate this term for ζ=0. The theoretical analysis for the additional –to the static and semi-static component– dynamic component of the load due to the Non Suspended Masses and the Suspended Masses of the vehicle, leads to the examination of the influence of the Non Suspended Masses only, since the frequency of oscillation of the Suspended Masses is much smaller than the frequency of the Non Suspended Masses. If m_{NSM} represents the Non Suspended Mass, m_{SM} the Suspended Mass and m_{TRACK} the Track Mass participating in the motion of the Non Suspended Masses of the vehicle, the differential equation is (with no damping ζ=0):

$$m_{NSM}\cdot\frac{d^2z}{dt^2}+h_{TRACK}\cdot z=m_{NSM}\cdot g\Rightarrow$$

$$\Rightarrow\left(m_{NSM}+m_{TRACK}\right)\cdot\frac{d^2z}{dt^2}+h_{TRACK}\cdot z=m_{NSM}\cdot g \quad (12)$$

where the track mass m_{TRACK} that participates in the motion of the Non Suspended (Unsprung) Masses of the Vehicles, ρ_{total} the total static stiffness coefficient of the track, ℓ the distance among the sleepers, E, J the modulus of elasticity and the moment of inertia of the rail, m_0 the unitary mass of track (per unit of length of the track).

For a comparison of the theoretical track mass to measurement results refer to [13]; [14]. The particular solution

of the differential Eqn (12) corresponds to the static action of the weight of the wheel:

$$z = \frac{m_{TRACK} \cdot g}{h_{TRACK}}$$

We assume that the rolling wheel runs over an isolated sinusoidal defect of length λ of the form:

$$n = \frac{a}{2} \cdot \left(1 - \cos\frac{2\pi x}{\lambda}\right) = \frac{a}{2} \cdot \left(1 - \cos\frac{2\pi V t}{\lambda}\right)$$

where n is the ordinate of the defect. Consequently, the ordinate of the center of inertia of the wheel is n+z. Defining τ1 as the time needed for the wheel to pass over the defect at a speed V:

$$\tau_1 = \frac{\lambda}{V} \quad , \quad \text{then:}$$

$$m_{NSM} \cdot \frac{d^2}{dt^2}(z+n) + m_{TRACK} \cdot \frac{d^2 z}{dt^2} + h_{TRACK} \cdot z = 0 \Rightarrow$$

$$\Rightarrow (m_{NSM} + m_{TRACK}) \cdot \frac{d^2 z}{dt^2} + h_{TRACK} \cdot z = -m_{NSM} \cdot \frac{d^2 n}{dt^2} =$$

$$= -m_{NSM} \cdot \frac{2a\pi^2}{\tau_1^2} \cdot \cos\frac{2\pi t}{\tau_1}$$

Since:

$$\frac{dn}{dt} = \frac{a}{2} \cdot \frac{2\pi V}{\lambda} \cdot \sin\frac{2\pi V t}{\lambda} = \frac{a}{2} \cdot \frac{2\pi\lambda}{\lambda \cdot \tau_1} \cdot \sin\frac{2\pi V t}{\lambda} \Rightarrow$$

$$\Rightarrow \frac{dn}{dt} = \frac{a}{2} \cdot \frac{2\pi}{\tau_1} \cdot \sin\frac{2\pi V t}{\lambda} \Rightarrow$$

Where: $x = V \cdot t, \quad \omega_1 = 2 \cdot \frac{\pi \cdot V}{\ell} = \frac{2\pi}{T}, \quad \omega_n^2 = \frac{h_{TRACK}}{m_{NSM}}$

and ω_1 the cyclic frequency of the external force and ω_n the natural frequency. The additional dynamic component of the load due to the motion of the wheel is:

$$-m_{NSM} \cdot (z'' + n'') = h_{TRACK} \cdot z + m_{TRACK} \cdot z'' \qquad (14)$$

To solve Eqn (12) we divide by (m_{NSM}+m_{TRACK}):

$$\frac{d^2 z}{dt^2} + \frac{h_{TRACK}}{(m_{NSM} + m_{TRACK})} \cdot z =$$

$$= -\frac{m_{NSM}}{(m_{NSM} + m_{TRACK})} \cdot \frac{2a\pi^2}{\tau_1^2} \cdot \cos\frac{2\pi t}{\tau_1} \qquad (15a)$$

The differential equation of motion, for an undamped forced harmonic motion is ([19]; [20]):

$$m \cdot \ddot{z} + kz = p_0 \cos(\omega_1 t) \Rightarrow$$

$$\Rightarrow \ddot{z} + \frac{k}{m} z = \frac{p_0}{m} \cos(\omega_1 t) = \omega_n^2 \cdot \frac{p_0}{k} \cos(\omega_1 t) \qquad (15b)$$

where:

$$\omega_n^2 = \frac{k}{m} \Rightarrow m = \frac{k}{\omega_n^2}$$

Eqn (15a) is quite the same as Eqn (15b). The complete solution is:

$$z(t) = \frac{p_0}{k} \cdot \frac{1}{1 - \left(\frac{\omega_1}{\omega_n}\right)^2} \cdot \left| \underbrace{\cos(\omega_1 t)}_{steady-state} - \underbrace{\cos(\omega_n t)}_{transient-part} \right| \qquad (16)$$

when: k=h_{TRACK}, m=m_{NSM}+m_{TRACK}, and:

$$\omega_n^2 = \frac{h_{TRACK}}{m_{NSM} + m_{TRACK}}, \quad p_0 = -\frac{2 \cdot \alpha \cdot \pi^2 \cdot m_{NSM}}{\tau_1^2}$$

The general solution of Eqn (15) is:

$$z(t) = -\underbrace{\frac{2 \cdot \alpha \cdot \pi^2 \cdot m_{NSM}}{\tau_1^2}}_{p_0} \cdot \frac{1}{h_{TRACK}} \cdot \frac{1}{1 - \left(\frac{\omega_1}{\omega_n}\right)^2} \cdot \left| \underbrace{\cos(\omega_1 t)}_{steady-state} - \underbrace{\cos(\omega_n t)}_{transient-part} \right| =$$

$$= \frac{\alpha}{2} \cdot \frac{m_{NSM}}{(m_{NSM} + m_{TRACK})} \cdot \frac{1}{1 - \left(\frac{\omega_n}{\omega_1}\right)^2} \cdot \left[\underbrace{\cos(\omega_1 t)}_{steady-state} - \underbrace{\cos(\omega_n t)}_{transient-part} \right] \quad \text{and}$$

$$z(t) = -\frac{1}{2} \cdot \underbrace{\frac{4 \cdot \pi^2}{\tau_1^2}}_{\omega_1^2} \cdot \frac{\alpha \cdot m_{NSM}}{\underbrace{\omega_n^2 \cdot (m_{NSM} + m_{TRACK})}_{h_{TRACK}}} \cdot \frac{1}{1 - \left(\frac{\omega_1}{\omega_n}\right)^2} \cdot \left| \underbrace{\cos(\omega_1 t)}_{steady-state} - \underbrace{\cos(\omega_n t)}_{transient-part} \right| =$$

$$= \frac{\alpha}{2} \cdot \frac{m_{NSM}}{(m_{NSM} + m_{TRACK})} \cdot \frac{1}{1 - \left(\frac{\omega_n}{\omega_1}\right)^2} \cdot \left[\underbrace{\cos(\omega_1 t)}_{steady-state} - \underbrace{\cos(\omega_n t)}_{transient-part} \right] \qquad (17)$$

where, $T_n = 2\pi/\omega_n$ the period of the free oscillation of the wheel circulating on the rail and $T_1 = 2\pi/\omega_1$ the necessary time for the wheel to run over a defect of wavelength λ: $T_1 = \lambda/V$. Consequently, $T_n/T_1 = \omega_1/\omega_n$.

From Eqn (17):

$$\frac{(m_{NSM} + m_{TRACK})}{m_{NSM}} \cdot z(t) =$$

$$= \alpha \cdot \frac{1}{2} \cdot \frac{1}{1 - \left(\frac{\omega_n}{\omega_1}\right)^2} \cdot \left[\underbrace{\cos(\omega_1 t)}_{steady-state} - \underbrace{\cos(\omega_n t)}_{transient-part} \right] \qquad (18)$$

We can investigate equation (18) after a sensitivity analysis by variating parameters: for given values of $T_n/T_1 = \omega_1/\omega_n$ and for given value of V (for example equal to 1) the time period T_1 is proportional to μ=0.1, 0.2, … 1.0 of defect λ (where λ is the defect's wavelength). Equation (18) is transformed:

$$\left[\frac{(m_{NSM} + m_{TRACK})}{m_{NSM}} \cdot z(t) \cdot \frac{1}{\alpha} \right] = \frac{1}{2} \cdot \frac{1}{1 - (n)^2} \cdot \left| \underbrace{\cos(\omega_1 t)}_{steady-state} - \underbrace{\cos(n \cdot \omega_1 t)}_{transient-part} \right| =$$

$$= \frac{1}{2} \cdot \frac{1}{1 - (n)^2} \cdot \left[\underbrace{\cos(2\pi \cdot \mu)}_{steady-state} - \underbrace{\cos(n \cdot 2\pi \cdot \mu)}_{transient-part} \right] \qquad (19)$$

where $n = \omega_n/\omega_1$, $\omega_1 = \lambda/V$ and we examine values of $\mu \cdot \lambda = 0, 0.1\lambda, 0.2\lambda, \ldots, 0.8\lambda, 0.9\lambda, \lambda$, for discrete values of $n = \omega_n/\omega_1$ ($= T_1/T_n$) and μ a percentage of the wavelength λ. In Figure 6 the equation (19) is depicted.

6. Measurement-base of Track Recordingvehicles/ Cars and Track-defects of Long Wavelength

The measurement-base (chord) of 10 m length, along a railway line, is very important because it includes the wavelengths of the vehicles' hunting, since normally the measurements' base in railway measuring vehicles is approximately 10 m; consequently for larger wavelengths the measured defects' values f(x)=d [from the measuring vehicles or track recording cars] are smaller than the real ordinates $z(x)=d_1$ of the defects (Fig. 6a).

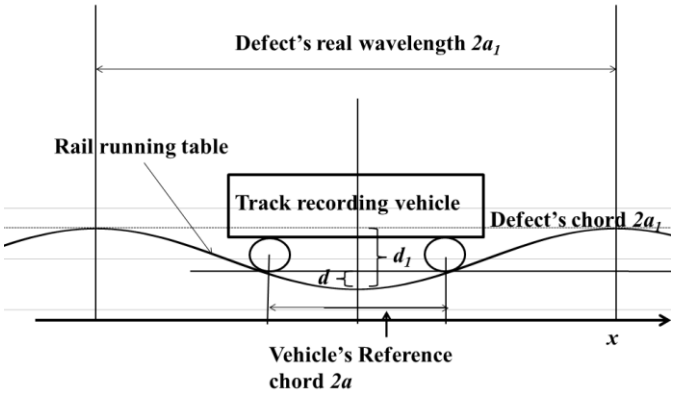

Fig. 6a Measurement of the ordinate d of a longitudinal vertical defect at the position x on a measurement-base (chord) of 2a length: 2a is much smaller than the defect's wavelength $2a_1$, consequently the measured value d is smaller than the real defect's depth (sagitta) d_1.

It should be clarified that different wavelengths address different vehicles' responses depending on the cord (different from 10 m). This is of decisive importance for the wavelengths of 30 – 33 m, which are characteristic for very High Speed Lines ([7], p.30, [21], [15], p.342). In the real tracks, the defects' forms are random with wavelengths from few centimetres to 100 m. Thus we should pass from the space-time domain to the frequencies' domain through the Fourier transform, in order to use the power spectral density of the defects (about spectral density of defects in a railway track see [3]). The total procedure for this is out of the scope of the present paper since it belongs to the domain of the measurements of track defects via track recording vehicles.

The defects of short wavelength exert important dynamic increments of the load on the track. If the speed V increases, the T1/Tn decreases and the supplementary subsidence, owed to the dynamic increase of the load, decreases too. We observe that when the speed overpasses the critical speed, for the defect that we investigate, when the rigidity of the track (stiffness) increases, Tn decreases and T_1/T_n increases and we approach the maximum-maximorum. For a defect of short wavelength the high rigidity (stiffness) is disadvantageous.

In the real tracks, the defects are random with wavelengths from few centimetres to 100 m. The defects constitute the "Input" in the system "Vehicle-Track" since the deflection y and the Action/Reaction R of each support point of the rail/sleeper are the "Output" or "Response" of the system. The accuracy of the measurements of the defects is of utmost importance for the calculation of the deflection y and the Reaction R; this accuracy, due to the bases of the measuring devices/vehicles, is fluctuating. Thus we should pass from the space-time domain to the frequencies' domain through the Fourier transform, in order to use the power spectral density of the defects (for the power spectral density see [3]; [6]), especially for defects, with (long) wavelength, larger than the measuring base of the vehicle.

We remind that for a function f(x) or y(x) [let's say the vertical defects' function, the input], its Fourier transform F(ω) is given by:

$$F(\omega)=\int_{-\infty}^{+\infty} f(t)\cdot e^{-i\omega t}\cdot dt,\quad with\quad i=\sqrt{-1},\quad and$$

$$f(t)=\frac{1}{2\pi}\cdot\int_{-\infty}^{+\infty} F(\omega)\cdot e^{i\omega t}\cdot dt \tag{20}$$

and:

$$F(\omega)=A(\omega)\cdot e^{[i\cdot\varphi(\omega)]}\cdot dt \tag{21}$$

where the graphic representation of the absolute value is called the Fourier spectrum of the f(t) and $|F(\omega)|^2$ is called the energy spectrum with φ(ω) the phase angle. *F(ω) or F(v)* is called the Fourier transform of the function *f(t)* or *y(t)*.

In the case of random defects then we do not use the function f(x) but its Fourier transform:

$$F(\Omega)=\int_{-\infty}^{+\infty} f(x)\cdot e^{-i\Omega x}\cdot dx \tag{22}$$

In practice we don't know the function of real defects y(x) but the measured values f(x) (see Eqns 23 below), from the recording vehicle, and we imply that:

$$S_Z(\Omega)=S_{INPUT}(\Omega)=\frac{S_F(\Omega)}{|K(\Omega)|^2}=\frac{S_{OUTPUT}(\Omega)}{|K(\Omega)|^2} \tag{24}$$

where $S_Z(\Omega)$ is the spectral density of the Fourier transform of the real defects (input in the track recording vehicle), $S_F(\Omega)$ is the spectral density of the Fourier transform of the measured values (output) and K(Ω) is a complex transfer function, called frequency response function, transforming the measured values of defects to the real values. For very High Speed Lines we should analyze the system "railway track – railway vehicle". The calculation of the spectrum of track defects is described in [3] (paragr. 6) and [6] (p.155-158).

7. Control of the Geometry of the Track: Measurements of the Defects by Track-recording Vehicles/Cars

Every point on each rail (at the rail running table) of a track can be defined by its three coordinates: at the position x and the functions y(x), in the horizontal alignment, and z(x), in the vertical alignment. The measurements of the defects are

performed with track geometry cars, the contact cars, which are made by actual contact with the rails, movable feeler points (transducers) that touch the rails to measure the parameters, e.g. the profile. The cars use the position of the car-body, its yaw and roll and, consequently their axles as the reference base for a relative measurement ([22, p.678-679]). We examine the vertical defect, the dip between two bumps, of an oscillograph recording ([22, p. 684]), as in Figure 1 (upper left), with a reference chord of length 2a (normally 10 m) and the reliability of the measurements. The value of d at the position x is:

$$d = f(x) = \frac{1}{2}\left[z(x-a) + z(x+a)\right] - z(x) \qquad (23a)$$

This transformation cannot be easily reversed: If we know z(x) in every x easily f(x) can be derived, but if we know f(x) it is not easy to calculate z(x). Thus we try to approach the matter for the case of a sinusoidal defect:

$z(x) = b \cdot \sin\frac{2\pi}{\ell}x$, we can derive that:

$$f(x) = \frac{1}{2}\cdot\left[b\cdot\sin\frac{2\pi}{\ell}(x-a) + b\cdot\sin\frac{2\pi}{\ell}(x+a)\right] - b\cdot\sin\frac{2\pi}{\ell}x =$$

$$= \frac{1}{2}\cdot b\cdot\sin\frac{2\pi}{\ell}(x-a) + \frac{1}{2}\cdot b\cdot\sin\frac{2\pi}{\ell}(x+a) - b\cdot\sin\frac{2\pi}{\ell}x =$$

$$= \frac{1}{2}\cdot b\cdot \left(\sin\frac{2\pi}{\ell}x\cdot\cos\frac{2\pi}{\ell}a - \cos\frac{2\pi}{\ell}x\cdot\sin\frac{2\pi}{\ell}a + \sin\frac{2\pi}{\ell}x\cdot\cos\frac{2\pi}{\ell}a + \cos\frac{2\pi}{\ell}x\cdot\sin\frac{2\pi}{\ell}a\right) -$$

$$-b\cdot\sin\frac{2\pi}{\ell}x \Rightarrow$$

$$\Rightarrow f(x) = -b\cdot\sin\left(\frac{2\pi}{\ell}x\right)\cdot\left(1-\cos\frac{2\pi}{\ell}a\right) =$$

$$= -z(x)\cdot\underbrace{\left(1-\cos\frac{2\pi}{\ell}a\right)}_{J(\Omega)} = -z(x)\cdot J(\Omega) \qquad (23b)$$

with $\Omega=2\pi/\ell$. $J(\Omega)$ is a real function and it is the transfer function, permitting to pass from z(x) to f(x). If the chord 2a is the chord used as base from the track recording vehicle then $J(\Omega)$ is the transfer function of the vehicle. The track recording vehicles measure the defects, the track displacement, "under load", that is under their axle load, which is usually smaller than the maximum axle load of the Railway-Line but enough for the measurement of the gaps under the seating surface of the sleepers, if any. Normally the chord used as reference base both for the vertical and horizontal defects is the 10 m length and the axles of the vehicle are used for that. Regarding the reliability of the measurements, three cases are distinguished:

(a) The vehicle's reference base 2a (chord of 10 m) is smaller than the defect's wave-length $\ell=2a_1$ (Fig. 6a). In that case the measured defect's ordinate f(x)=d is much smaller than the real defect's ordinate $z(x)=d_1$.

(b) The chord 2a is equal to the defect's wavelength $\ell=2a_1$, and $f(x)=d=z(x)=d_1$ (Fig. 6d).

(c) The chord 2a is larger than the defect's wavelength $\ell=2a_1$, with the reliability fluctuating. The most characteristic case happens when the defect's wavelength ($2a_1$) equal to ½ of the chord's length (2a) and the measured ordinate f(x)=d=0 instead of the real defect's ordinate $z(x)=d_1$ (Fig. 6c).

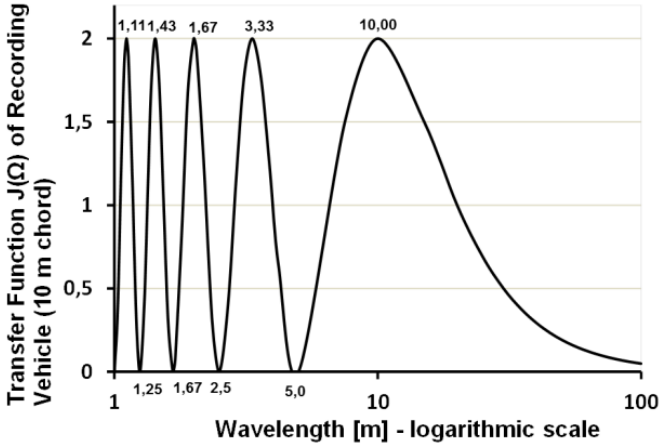

Fig. 6b Measurement of a longitudinal vertical defect at the position x on a chord of 2a length: the reliability of track recording vehicle's measurements is depicted through its Transfer Function J(Ω).

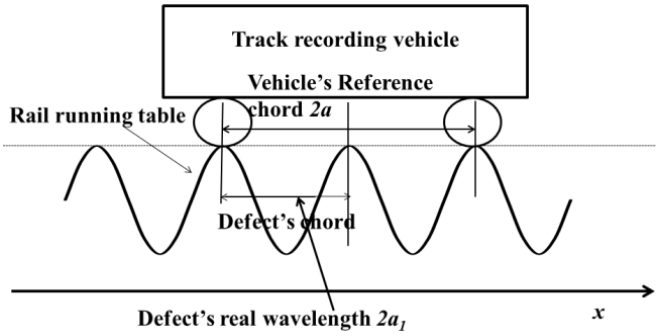

Fig. 6c Measurement of a longitudinal vertical defect at the position x on a chord of 2a length: 2a is double of the defect's wavelength $2a_1$.

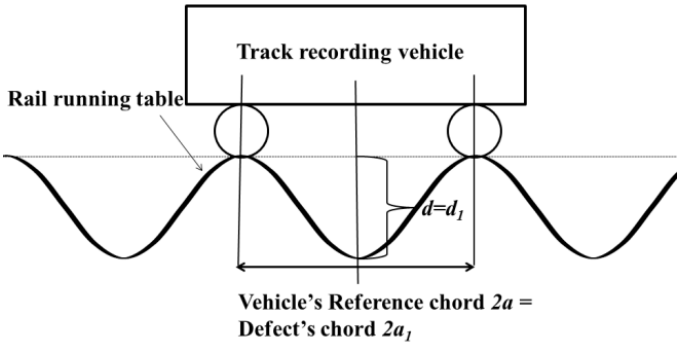

Fig. 6d Measurement of a longitudinal vertical defect at the position x on a chord of 2a length: 2a is equal to the defect's wavelength $2a_1$.

In order to approach the matter of the reliability of the measured values, by the track recording vehicle, we examine its transfer function $J(\Omega)$, presenting minimums, zero, for:

$$\frac{2\pi a}{\ell} = 2k\pi \Rightarrow \ell = \frac{a}{k} \quad (25)$$

with k integer and maximums equal to 2 for:

$$\frac{2\pi a}{\ell} = (1+2k)\cdot\pi \Rightarrow \ell = \frac{2a}{1+2k} \quad (26)$$

and in the case of a reference base (chord) of 10 m, that is a=10 m, then the values of J(Ω):

$$\frac{f(x)}{z(x)} = \frac{d}{d_1} = 0, \quad for$$

$$\ell = 5m,\ 2.5m,\ 1.67m,\ 1,25m,\ 1,00m \quad and \quad (27)$$

$$\frac{f(x)}{z(x)} = \frac{d}{d_1} = 2, \quad for$$

$$\ell = 10m,\ 3.33m,\ 2m,\ 1,42857m,\ 1,1111m \quad (28)$$

as depicted in Fig. 6b. The 10 m chord is very important because it includes the wavelengths of the vehicles' hunting, but for larger wavelengths the measured values f(x)=d are smaller than the real ordinates z(x)=d_1 (Fig. 6a). It should be clarified that different wavelengths address different vehicles' responses depending on the cord (different from 10 m). This is of decisive importance for the wavelengths of 30 – 33 m, that are characteristic for very High Speed Lines ([7, p.30], [21], [15, p.342]): for 30 m, J(Ω)=0.5 and for 50 m J(Ω)=0.2 (as we saw in the previous paragraph. *In any case, for each vehicle its reference chord should be used instead of the 10 m chord*.

In the real tracks, the defects are random with wavelengths from few centimeters to 100 m. Thus we should pass from the space-time domain to the frequencies' domain through the Fourier transform, in order to use the power spectral density of the defects. We remind that for a function f(x), its Fourier transform F(ω) is given by:

$$F(\omega) = \int_{-\infty}^{+\infty} f(t)\cdot e^{-i\omega t}\cdot dt, \quad with \quad i = \sqrt{-1}, \quad and$$

$$f(t) = \frac{1}{2\pi}\cdot\int_{-\infty}^{+\infty} F(\omega)\cdot e^{i\omega t}\cdot dt, \quad and \quad (29)$$

$$F(\omega) = A(\omega)\cdot e^{[i\cdot\varphi(\omega)]}\cdot dt \quad (30)$$

where the graphic representation of the absolute value $|F(\omega)| = A(\omega)$ is called the Fourier spectrum of the f(t) and $|F(\omega)|^2$ is called the energy spectrum with φ(ω) the phase angle.

In the case of random defects then we do not use the functions f(x) and z(x) but their Fourier transforms:

$$R[F(\nu)] = \int_{-\infty}^{+\infty} y(t)\cdot\cos(2\pi\nu t)\cdot dt \qquad real-part$$

$$F(\Omega) = \int_{-\infty}^{+\infty} f(x)\cdot e^{-i\Omega x}\cdot dx \quad (31)$$

Applying the Fourier transforms in the above equations (1) and (2) we find:

$$F(\Omega) = -Z(\Omega)\cdot\left[1-\frac{1}{2}\cdot\left(e^{i\Omega a}+e^{-i\Omega a}\right)\right] =$$

$$= -Z(\Omega)\cdot[1-\cos(\Omega\cdot a)] = -Z(\Omega)\cdot K(\Omega) \quad (32)$$

similar to equation (23b), but for the Fourier transforms of f(x) and z(x). In practice we don't know the real defect's function z(x) but the measured values f(x), from the recording vehicle, and from the equation (32) we imply that:

$$Z(\Omega) = \int_{-\infty}^{+\infty} z(x)\cdot e^{-i\Omega x}\cdot dx, \quad and \quad (33)$$

where $S_Z(\Omega)$ is the spectral density of the Fourier transform of the real defects (input in the track recording vehicle), $S_F(\Omega)$ is the spectral density of the Fourier transform of the measured values (output) and K(Ω) is a complex transfer function, called frequency response function, transforming the measured values of defects to the real values. As it was mentioned in the previous paragraph, for the very High Speed Lines we should analyze the system "railway track – railway vehicle".

8. The Fourier Transform and the Spectrum of Amplitudes and Phases in the System "Vehicle-track"

Before we examine any signal, waveform, random excitation, we should first bear in mind that there are two possible mathematical representations of this signal:

(a) a representation of the form y = f(t) for which the independent variable is the time t which elapses, and

(b) a frequency representation of the form Y = F(ν) for which the independent variable is frequency ν, whose unit is sec^{-1}, that is inverse of time.

These two mathematical representations are related through the Fourier transform and its inverse transform as given by the Eqn (20) and (21).

Figure 7 below gives an idea of the physical realization of the Fourier transform.

As analyzed in [6] (chapter III, paragraph 9), we can move from periodical to non-periodical excitation functions by «extension» of the period of the periodic (or harmonic) function to infinity: T → ∞. Hence, the interval of frequencies ν=1/T tends to zero and the spectral frequency function can be a continuous function.

F(ω) or F(Ω) or Y(ν) is a function of frequencies ν, which is a complex function in its general form, and contains a real and an imaginary part.

$$S_Z(\Omega) = S_{INPUT}(\Omega) = \frac{S_F(\Omega)}{|K(\Omega)|^2} = \frac{S_{OUTPUT}(\Omega)}{|K(\Omega)|^2}$$

$$R\left[F(\nu)\right]=\int_{-\infty}^{+\infty} y(t)\cdot\cos(2\pi\nu t)\cdot dt \qquad real-part$$

$$I\left[F(\nu)\right]=\int_{-\infty}^{+\infty} y(t)\sin(2\pi\nu t)\cdot dt \qquad imaginary-part$$

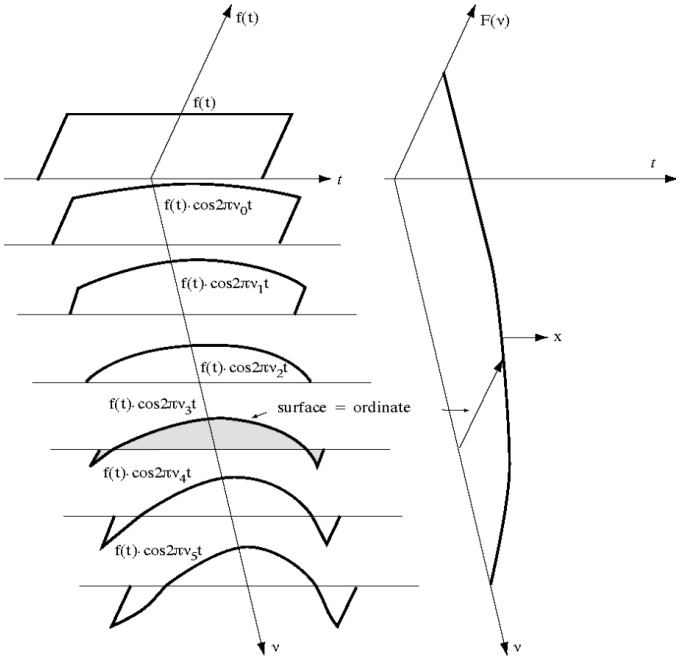

Fig. 7. Physical realisation of the Fourier transform ([6]).

The spectrum of the amplitudes is:

$$\left|F(\nu)\right|=\sqrt{\left[R\left[F(\nu)\right]\right]^2+\left[I\left[F(\nu)\right]\right]^2}$$

The spectrum of the phases are:

$$\varphi(\nu)=\arctan\left|-\frac{I\left[F(\nu)\right]}{R\left[F(\nu)\right]}\right|$$

From the above, we may conclude that in the case of non-periodic functions, the Fourier transform is a continuous frequency function. *In Eqns (20) and (21), functions F(ν) or F(ω) and f(t) or y(t) represent the same physical phenomenon, but through different presentation*. If we consider the function f(t), the point of the system that is being examined moves within the domain «amplitude-time». If we consider the function F(ω), the point of the system that is being examined moves within the domain «amplitude-frequency». The first function gives the image of the object under investigation (e.g. structure) in dimensions of space and time and the other one in dimensions of frequencies and amplitudes.

When we investigate F(ν) for a specific value ν_i of ν, this means that we examine its whole history, up to the present, but also to the future of f(t), to find whatever corresponds to frequency ν_i. This corresponds to an infinitesimally selective filtering. This filtering cannot take place under a physical process. Hence we cannot determine F(ν) with perfect accuracy for a specific ν_i, in the frequency axis.

In the same way, if we go on to f(t), starting from F(ν), we have to know the spectrum for all the frequencies up to infinity and the formula shows that the same operation of infinitesimally selective filtering intervenes, since the variables of time and frequency are interchangeable. This means that in order to determine the exact value of f(t) at an instance t, we must have and examine a frequency zone that tends to infinity. This is another form of the uncertainty principle that expresses «the weakness of man as an observer to understand reality without decomposing it or rendering it, in any way, "blurred" (see [23, p.23]). We remind the uncertainty principle of Heisenberg, according to which, neither the momentum nor the position of a particle inside the nucleus of an atom can be determined at the same time, with any great accuracy. On the contrary, the uncertainties for the two quantities have complementary roles. If position coordinate x of the particle has uncertainty Δx, as defined in this way, and if the corresponding linear momentum coordinate p_x has uncertainty Δp_x, then the two uncertainties relate to each other through the inequality $\Delta x \cdot \Delta p_x \geq R/2\pi$ ([24, p.1149]). The more precisely we determine the position, the more uncertain is the determination of the linear momentum, and vice versa.

9. Sensitivity Analysis for Track-defects in a High Speed Line

9.1 General

The first term in the bracket of Eqn (19) is depicted on the horizontal axis while on the vertical axis the percentages of the wavelength μ·λ are shown. We observe that z(x) has its maximum value for T_l/T_n=0,666667=2/3, equal to 1,465:

$$z(t)=\left|\frac{m_{NSM}}{\left(m_{NSM}+m_{TRACK}\right)}\right|\cdot\alpha\cdot 1{,}465 \qquad (34)$$

for x=0,91λ. The relation T_l/T_n represents the cases for short and long wavelength of the defects. For T_l/T_n=2-2,5 the wavelength is long and for T_l/T_n << the wavelength is short ([7, p.49]). The second derivative of z(x) from Eqn (17), that is the vertical acceleration that gives the dynamic overloading due to the defect (i.e. *the dynamic component of the total Load of the wheel*), is calculated:

$$z'(t)=\frac{\alpha}{2}\cdot\frac{m_{NSM}}{\left(m_{NSM}+m_{TRACK}\right)}\cdot\frac{1}{1-\left(\frac{\omega_n}{\omega_l}\right)^2}\cdot\left|\underbrace{-\omega_l\cdot\sin(\omega_l t)}_{steady-state}+\underbrace{\omega_n\cdot\sin(\omega_n t)}_{transient-part}\right| \qquad (35a)$$

$$z''(t)=-\frac{\alpha}{2}\cdot\frac{m_{NSM}}{\left(m_{NSM}+m_{TRACK}\right)}\cdot\frac{1}{1-\left(\frac{\omega_n}{\omega_l}\right)^2}\cdot\left|\underbrace{\omega_l^2\cdot\cos(\omega_l t)}_{steady-state}-\underbrace{\omega_n^2\cdot\cos(\omega_n t)}_{transient-part}\right| \qquad (35b)$$

for discrete values of $n=\omega_n/\omega_l$ ($=T_l/T_n$) and μ a percentage of the wavelength λ, and T_n=0,0307 sec as calculated above. The additional subsidence of the deflection z at the beginning of the defect is negative in the first part of the defect. Following the wheel's motion, z turns to positive sign and reaches its maximum and possibly afterwards z becomes again negative.

After the passage of the wheel over the defect, one oscillation occurs which approaches to the natural cyclic frequency ω_n (this oscillation is damped due to non-existence of a new defect since we considered one isolated defect) in reality, even if in the present analysis the damping was omitted for simplicity. The maximum value of ζ is given in Table 1 below, as it is –graphically– measured in Fig. 8.

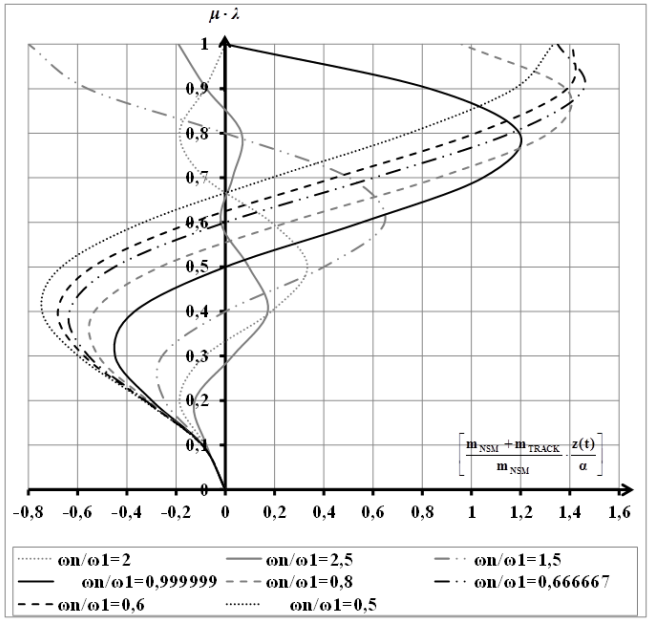

Fig. 8. Mapping of Eqn (19). On the Vertical Axis the percentage of the wavelength λ of the defect is depicted. On the Horizontal Axis the first term of Eqn (19), inside the brackets, is depicted.

Table 1: Maximum Values of ζ

T_1/T_n	2,5	2	1,5	1	0,8	0,66667	0,6	0,5
ζ	0,18	0,335	0,65	1,205	1,415	1,47	1,43	1,34
where: $\zeta=[(m_{NSM}+m_{TRACK})/m_{NSM}]\cdot[z_{max}/\alpha]$								

9.2 the Case of Short-wavelength Defects

It is observed that the maximum value:

$$\left[\frac{(m_{NSM}+m_{TRACK})}{m_{NSM}}\cdot\frac{z_{max}}{\alpha}\right]$$

is shifted towards the end of the defect as the ratio T_1/T_n decreases, that is when the defect's wavelength becomes short. The maximum is obtained for T_1/T_n = 0,666667 = 2/3. For each combination of "vehicle + track section", the critical value of the speed V, for which the 2/3 are achieved is a function of the wavelength λ. Since:

$$T_1=\frac{\lambda}{V}\Rightarrow V=\frac{\lambda}{T_1}=\frac{3}{2}\cdot\frac{\lambda}{T_n}$$

we can calculate the critical speed $V_{critical}$ for any combination of track layers and their corresponding stiffness. As a case study we use the ballasted track depicted in Fig. 4, for high speed, equipped with rail UIC60 (ρ_{rail} = 75.000 kN/mm), monoblock sleepers of prestressed concrete B70 type ($\rho_{sleeper}$ = 13.500 kN/mm), W14 fastenings combined with pad Zw700 Saargummi (ρ_{pad} fluctuating from 50,72 to 48,52 kN/mm), ballast fouled after 2 years in circulation ($\rho_{ballast}$ = 380 kN/mm) and excellent subgrade/substructure for high speed lines: $\rho_{subgrade}$ = 114 kN/mm [e.g. the New Infrastructure (NBS) of the German Railways]. These parameters' data are the ones measured on track by the German State Railways (DB), as cited in [7] and [18]. The calculation of the static stiffness coefficient of the subgrade ρ_{pad} for a high speed line of this type, as it is derived from the load-deflection curves of the pads provided by the producer, by the trial-and-error method described in [6, ch. 9]; see also [25] and [26]. For this cross section of ballasted track, h_{TRACK} is equal to 85,396 kN/mm = 8539,6 t/m and m_{TRACK} is equal to 0,426 t (for the calculations see [14]; [13]). If we consider an average m_{NSM}=1,0 t, then:

$$m_{NSM}+m_{TRACK}=\frac{1,0+0,426}{9,81}=0,145\qquad tons-mass$$

Where g = 9,81 m/sec^2, the acceleration of gravity. The period T_n is given by:

$$T_n=2\pi\sqrt{\frac{1,0+0,426}{9,81\cdot 8539,6}}=0,026\ \text{ sec}\Rightarrow$$

$$\Rightarrow V_{critical}=\frac{3}{2}\cdot\frac{\lambda}{T_n}=\frac{3}{2}\cdot\frac{\lambda}{0,026}=57,69\cdot\lambda$$

where an average h_{TRACK}=8539,6 t/m is used and $V_{critical}$ is given in [m/sec], λ in [m]. For a wavelength of 1,0 m, $V_{critical}$ = 57,69 m/sec = 207,7 km/h.

9.3 the Case of Long Wavelength Defects

If, now, we consider a long wavelength defect with a wavelength that produces a forced oscillation with:

$$\frac{T_1}{T_n}=\frac{\omega_n}{\omega_1}=2,5$$

we calculate (in Fig. 8 is 0,19, for x=0,41·λ):

$$z_{\max}=\left[\frac{m_{NSM}\cdot\alpha\cdot 0,19}{(m_{NSM}+m_{TRACK})}\right]=0,133\cdot\alpha$$

with the values calculated above: Tn = 0,026 sec, T1 = 0,065 sec, the wavelength λ equals:

$$\lambda=V\cdot T_1=2,5\cdot V\cdot T_n=0,065\cdot 57,69=3,75m$$

This value represents a defect of adequately long wavelength. The static deflection due to a wheel load of 11,25 t or 112,5 kN is equal to:

$$z_{static}=\frac{Q_{wheel}}{2\sqrt{2}}\cdot\sqrt[4]{\frac{\ell^3}{EJ\rho_{total}^3}}=\frac{112.500N}{2\sqrt{2}}\cdot$$

$$\cdot\sqrt[4]{\frac{600^3\,mm^3}{210.000\frac{N}{mm^2}\cdot 3{,}06\cdot 10^7 mm^4\cdot 85.396^3\frac{N^3}{mm^3}}}=$$

$$=\frac{112.500N}{2\sqrt{2}}\cdot 1{,}524228617\cdot 10^{-5}\frac{mm}{N}=0{,}606mm$$

Consequently, for α=1 mm, that is for every mm of vertical defect, the dynamic increment of the static deflection is equal to (0,133/0,606)=21,9% of the static deflection (for every mm of the depth of the defect).

If we examine the second derivative (vertical acceleration) as a percentage of g, the acceleration of gravity, then [from Eqns (35)]:

$$\left[\frac{\left(m_{NSM}+m_{TRACK}\right)}{m_{NSM}}\cdot\frac{z''(t)}{\alpha}\right]=-\frac{1}{2}\cdot\frac{\omega_1^2}{1-\left(\frac{\omega_n}{\omega_1}\right)^2}\cdot$$

$$\cdot\left[\underbrace{\cos\left(\frac{2\pi V}{\lambda}\cdot\frac{\mu\cdot\lambda}{V}\right)}_{steady-state}-\underbrace{\frac{\omega_n^2}{\omega_1^2}\cdot\cos\left(n\cdot\frac{2\pi V}{\lambda}\frac{\mu\cdot\lambda}{V}\right)}_{transient-part}\right]= \qquad (36)$$

$$=-\left(\frac{2\pi}{n\cdot T_n}\right)^2\cdot\frac{1}{g}\cdot\left|\frac{1}{2\cdot\left[1-(n)^2\right]}\cdot\left|\underbrace{\cos(2\pi\mu)}_{steady-state}-\underbrace{(n)^2\cdot\cos(2n\pi\mu)}_{transient-part}\right|\right|$$

and the result is a percentage (%) of g.

Equation (36) is plotted in Fig. 9.

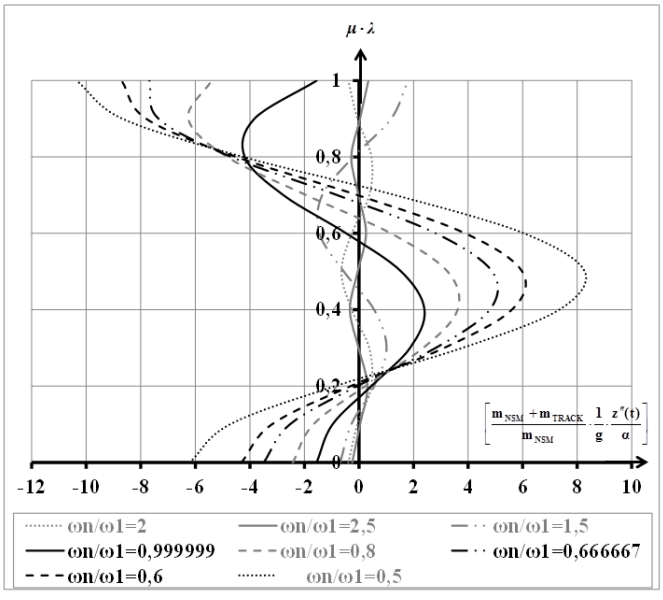

Fig. 9. Mapping of the Eqn (36), for the vertical acceleration due to a defect of long wavelength. In the Vertical Axis the percentage of the wavelength λ of the defect is depicted. In the Horizontal Axis the first term of Eqn (36), in the brackets, is depicted.

The first term in the bracket of Eqn (36) is depicted on the horizontal axis while on the vertical axis the percentages of the wavelength μ·λ are shown. For the case calculated above in Fig. 9, at the point x=0,41·λ the term in bracket has a value of -0,332:

$$\left[\frac{\left(m_{NSM}+m_{TRACK}\right)}{m_{NSM}}\cdot\frac{1}{g}\cdot\frac{z''(t)}{\alpha}\right]=-0.332041\Rightarrow z''(t)=$$

$$=-0.332041\cdot\frac{1{,}0}{1{,}0+0{,}426}\cdot g\cdot\alpha=0{,}233\cdot g\cdot\alpha$$

Eqn (12) (its second part corresponds to the static action of the wheel load) has as particular solution:

$$z=\frac{m_{NSM}\cdot g}{h_{TRACK}}$$

Abandoning the second part leads to the classic solution where z is the supplementary subsidence owed to the dynamic increase of the Load. The dynamic increase of the Load is equal to:

$$Q_{dynamic}=h_{TRACK}\cdot z+m_{TRACK}\cdot z''=85.396\cdot 0{,}133-$$

$$-426kg\cdot 0{,}233\cdot 9{,}81\frac{m}{\sec^2}=1{,}04t \qquad (37)$$

where, from the analysis above: h_{TRACK} = 8539,6 t/m = 85.396 N/mm, m_{TRACK} = 0,426 t = 426 kg. Consequently, for arc height (i.e. sagitta) α=1 mm of a defect of wavelength λ, that is for every mm of vertical defect, the dynamic increase of the load is equal to (1,04/ 11,25)=9,24% of the static load of the wheel (for every mm of the depth of the defect). Apparently the increase of the static stiffness coefficient and of the inferred dynamic stiffness coefficient of track leads to lower values of $Q_{dynamic}$ since the h_{TRACK} is in the denominator in the equation for calculation of z, consequently the first term of the Eqn (35b) for the dynamic overloading due to a defect (i.e., the dynamic component of the total Load of the wheel) will be reduced. The same happens for the track mass participating in the motion of the Non Suspended Masses of the wheel. Thus finally the $Q_{dynamic}$ will be reduced when the ρ_{total} and the h_{TRACK} are increased.

In the case of a defect of long wavelength, when the speed V increases, then T_1 decreases and the supplementary subsidence, owed to the dynamic increase of the load, increases; consequently the dynamic component of the load due to the Non Suspended Masses increase more rapidly since it depends on $(\omega_1)^2$, that is on the square of the speed V. When the dynamic rigidity h_{TRACK}=ρdynamic increases, then the eigenperiod Tn decreases and T1/Tn increases and the supplementary subsidence, owed to the dynamic increase of the load, decreases for the same speed V; one higher rigidity (stiffness coefficient) is still advantageous. For defects of longer wavelength, the oscillations of the Suspended Masses become predominant since the oscillations of the Non

Suspended Masses decrease.

The results presented so far and the arithmetic comparisons give an idea and enlighten the influence of some kinds of track defects as well as of several parameters, but the calculations do not take into account the amortization of the oscillations due to the damping of the track and mainly of the ballast, consequently the derived arithmetic values are larger than the real values. For example in the case of the theoretical calculation of the track mass which participates in the motion of the Non Suspended Masses of the railway vehicles without damping give results 33% larger than the real ones since if we take into account the damping coefficient of the track the variation between the results of the theoretical calculations and the real values measured on track fluctuates between 0,5 and 4% ([14]; compared to [13]), fact depicting the accuracy of the theoretical calculations, if the totality of the parameters is taken into account.

10. Conclusions

In order to approach the matter of the reliability of the measured values of the track-defects by the track recording vehicles/cars, we should examine the transfer function of the recording vehicle which presents minimums and zero-points. In the real conditions, the defects are random with wavelengths from few centimeters to 100 m. Since the length of the vehicle's measuring base is much shorter than 100 m, we should pass from the space-time domain to the frequencies' domain through the Fourier transform, in order to use the power spectral density of the defects. Furthermore, in the case of random defects, we cannot and do not use the functions f(x) and z(x) but we can use their Fourier transforms.

For a defect of long wavelength λ and sagitta of 1 mm (depth of the defect), the dynamic increase of the acting load – compared to the static wheel load– is equal to 9,24%. Furthermore from Fig. 8 and Fig. 9, it is verified that when the speed increases, the period T_1 decreases and the supplementary sagitta (depth of the defect) increases. Supplementary (sagitta), since it is added to the static deflection and it is owed to the dynamic component of the load. The increase of the dynamic component of the load increases faster since it is dependent on the square of the speed $(\omega_1)^2$. When the dynamic stiffness coefficient h_{TRACK} increases, T_n decreases, T_1/T_n increases, the supplementary sagitta decreases (for the same V), and the dynamic component of the action decreases also. Furthermore, in the case of longer wavelengths the oscillations of the Suspended Masses become predominant since the oscillations of the Non Suspended Masses decrease.

Consequently, the softer the pad and/or the subgrade (subgrade and prepared subgrade) then the higher percentage of the load is transmitted through the sleeper to the substructure of the railway track under the running load/axle. Finally in total, the reaction per support point of the rail/sleeper, in the case of softer pads and more resilient fastenings, is smaller due to a distribution of the load along the track in more support points of the rail/sleepers, as it can be derived from literature ([1]; [6]; [2]). In the case of the short wavelength defects this is more clearly verified.

It should be clarified that different wavelengths address different vehicles' responses depending on the measurement-base/cord (different from 10m). This is of decisive importance for the wavelengths of 30 – 33 m, which are characteristic and of very high-impact in the case of very High Speeds.

For defects of very long wavelength, the oscillations of the Suspended Masses (strongly influencing the feeling of "passenger-comfort") become predominant, since the oscillations of the Non Suspended Masses decrease (strongly influencing the Loading of the Track): in the case of long wavelength defects, when the speed V increases, then T_1 decreases and the supplementary subsidence, owed to the dynamic increase of the load, increases; consequently the dynamic component of the load due to the Non Suspended Masses increase more rapidly since it depends on $(\omega_1)^2$, that is on the square of the speed V.

References

[1]. K. Giannakos, A. Loizos: Evaluation of actions on concrete sleepers as design loads – Influence of fastenings, International Journal of Pavement Engineering (IJPE), Vol. 11, Issue 3, June, 197 – 213, (2010).

[2]. K. Giannakos: Loads on track, Ballast Fouling and Life-cycle under Dynamic Loading in Railways, International Journal of Transportation Engineering – ASCE, Vol. 136, Issue 12, 1075-1084, (2010a).

[3]. K. Giannakos: Modeling the Influence of Short Wavelength Defects in a Railway Track on the Dynamic Behavior of the Non-Suspended Masses, Journal Mechanical Systems and Signal Processes (jmssp), Elsevier, 68-69, (2016), 68-83, http://dx.doi.org/10.1016/j.ymssp.2015.07.020, (2015).

[4]. E. Winkler: Die Lehre von der Elastizität und Festigkeit (The Theory of Elasticity and Stiffness), H. Dominicus, Prague, (1867).

[5]. H. Zimmermann: Die Berechnung des Eisenbahnoberbaues, Verlag von Wilhelm Ernst & Sohn, Berlin, (1941).

[6]. K. Giannakos: Actions on the Railway Track, Papazissis publications, Athens, Greece, http://www. papazisi.gr, (2004).

[7]. J. Alias: La Voie Ferree, IIeme edition, Eyrolles, Paris, (1984).

[8]. J. Eisenmann: Schotteroberbau – Moglichkeiten und Perspektiven fur die Moderne Bahn, Die Naturstein-Industrie, Heft 3, (Isernhagen, Germany), 6-11 (1988).

[9]. K. Giannakos: Ties' Design in High -Speed and Heavy Haul Railroads: Ultimum Strength vs Actions on Track, presented in the workshop for sleepers and

fastenings of TRB (2013a), 92nd Annual Meeting, proceedings.

[10]. K. Giannakos: Selected Topics in Railway Engineering, University of Thessaly, Dpt. Civil Engineering, Greece, www.uth.gr, (2013b).

[11]. H. Jenkins, J. Stephenson, G. Clayton, G. Morland, D. Lyon: Incidences des parametres carac-teristigues de la voie et des vehicules sur les efforts dynamigues verticaux gui se developpent entre rail et roue, Rail International 10/(1974), 682-702.

[12]. SNCF: Mecanique de la voie, (1981).

[13]. K. Giannakos: Theoretical calculation of the track-mass in the motion of unsprung masses in relation to track dynamic stiffness and damping, International Journal of Pavement Engineering (IJPE) - Special Rail Issue: "High-Speed Railway Infrastructure: Recent Developments and Performance", Vol. 11, number 4, p. 319-330, August, (2010b).

[14]. K. Giannakos: Influence of the Track's Damping on the Track Mass Participating in the Motion of the Non Suspended Masses of Railway Vehicles- Theoretical Calculation and Comparison to Measurements, volume published in honor of professor G. Giannopoulos, Aristotle University of Thessaloniki, (2012).

[15]. J. Fortin: La Deformee Dynamique de la Voie Ferree, RGCF, 02/1982.

[16]. D. Thompson: Railway Noise and Vibration, Elsevier, 2009.

[17]. SNCF/Direction de l' Equipement: Mecanique de la Voie, Paris, (1981).

[18]. A. Prud'homme: Sollicitations Statiques et Dynamiques de la Voie, SNCF/ Direction des Installations Fixes, Paris, (1969/ 1966).

[19]. A. Chopra: Dynamics of Structures – Theory and Applications to Earthquake Engineering, Prentice Hall, second edition, USA, (2001).

[20]. J. Argyris, H.-P. Mlejnek: Texts on Computational Mechanics, Volume V Dynamics of Structures, North-Holland, Elsevier, New York, USA, (1991).

[21]. OSE/SNCF, Cooperation: Comportment des traverses en relation avec les charges dynamiques, June, (1988).

[22]. W. Hay: Railroad Engineering, John Wiley & Sons, USA (1982).

[23]. J. Max: Methodes et Techniques de Traitement du Signal et Applications aux Measures Physiques, Masson, Paris, (1985).

[24]. Hugh J. Young: Physics, Greek edition, vols I, II, Papazisis publications, Athens, 1994; Addison-Wesley, 1992.

[25]. K. Giannakos, S. Tsoukantas, A. Sakareli, C. Zois: Schwankung des Steifigkeit zwischen Fester Fahrbahn und Schottergleis - Beschrieben wird die parametrische Analyse der Schwankung des Steifigkeitsfaktors im Übergangsbereich zwischen Fester Fahrbahn und Schottergleis, EI - Eisenbahningenieur, Germany, February 2011, 12-19, (2011).

[26]. K. Giannakos, S. Tsoukantas: Requirements for Stiffness Variation between Slab and Ballasted Railway Track and Resulting Design Loads, ICASTOR (Indian Centre For Advanced Scientific and Technological Research) Journal for Engineering, January 2010, Vol.3, No 1 (2010), p. 21 - 35, (2010).

Creative Commons Attribution License 4.0 (Attribution 4.0 International, CC BY 4.0)